Experiments on Rockfall Protection Embankments with Geogrids and Cushions

Int. J. of GEOMATE , Oct. 2011, Vol. 1, No.1 (Sl. No. 1), pp. 19-24
Geotec., Const. Mat. and Env., ISSN:2186-2982(P), 2186-2990(O), Japan

Experiments on Rockfall Protection Embankments with Geogrids and Cushions

Koji Maegawa, Department of Environmental Design, Kanazawa University
Tetsuya Yokota, Raiteku Co. Ltd.
Phuc Tran Van, Graduate School of Natural Science & Technology, Kanazawa University

ABSTRACT: There are various protection measures against rockfalls. An embankment is effective in rockfall hazard mitigation at a dangerous slope end. The slope rockfall tests on full-scale embankments have been carried out. These embankments are made of sandy soil reinforced with geogrids. The cushioning layers which are made of geocells filled with crushed stones of 5-13 mm in diameter are also placed on the mountain side of the embankment. A boulder, i.e., RC block rolls down the test-site slope, and hits against the embankment. A new system of measuring instruments is employed in order to evaluate the impact force and the impact energy. One of important observations is a possibility that a rolling boulder carries it toward the top of an embankment because of its rolling momentum. The experimental results, especially the relationship between impact force and impact energy is discussed in this paper.

Keywords: rockfall, embankment, geogrid, experiment

1. INTRODUCTION

Mitigation measures against natural hazards such as rockfalls, avalanches, and shallow landslides are important subjects in mountainous areas. Various structures such as snowsheds, rocksheds, net fences, and rope barriers are constructed in order to protect infrastructures, housing, and lives in such regions. Many full-scale tests of these structures have been carried out and their design methods and schemes have been presented. In particular, JRA [1] gave some design examples. Gerber [2] and ETAG-027 [3] set forth guidelines for the technical approval of rockfall protection kits, principally net fences.

As shown in Fig. 1, an embankment is an embankment is a rock barrier that has the advantage of lower construction and repair costs and the capacity to absorb impact energy higher than the other barriers, although it requires a suitable construction site. The design method for embankments is based roughly on empirical solutions obtained from full-scale tests because of the complicated dynamic and plastic behavior of sandy soil.

Though the number of full-scale tests is limited, many researchers have carried out tests on embankments reinforced with geosynthetics [4]. Burroughs [5] and Obata [6] used rock blocks which had different shapes, sizes, and weights and rolled down an actual slope against embankments. In this case, the movement of the test bkocks is uncertain; therefore, it is not easy to effectively aim a falling rock at a target on an embankment. The test blocks may also break as they roll. Peila [4], [7] made reinforced concrete (RC) blocks weighing up to 9000 kg and used a cableway device that was able to accurately throw the blocks with a speed of 32 m/s at a target on an embankment. Impact energy has been estimated using the kinetic energy of rockfall movement whose velocity has been probably measured by a high-speed camera, but the impact force resisted by the embankments has not been reported in these papers.

In this investigation, the slope rockfall tests was conducted on full-scale embankments reinforced with geogrids and protected by cushion layers. The purpose of the tests was to confirm the behavior of reinforced embankments subjected to the impact of a realistic slope rockfall, and consequently to define the allowable energy levels for the structures to ensure safe and/or repairable conditions. The steel-covered RC blocks weighing up to 17.1 ton were used instead of boulders. The motion and impact force of the RC blocks were measured during the fall and impact. The experimental result, especially the relationship between impact force and impact energy is discussed in this paper.

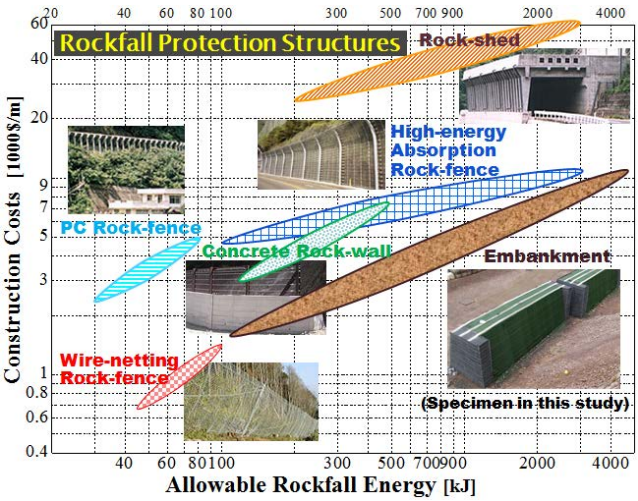

Fig. 1 Construction costs for rockfall protection structures

2. OUTLINE OF SLOPE-ROCKFALL TESTS

2.1 Slope Features of Test Site

The tests were carried out in a quarry near Uonuma city in northern Japan. At the site, two feasible rock-slope lanes 37 m high with a slope of 42 degrees are available for rolling RC blocks down the slope as shown in Fig. 2. The RC blocks were individually launched by a backhoe to roll down the slope.

2.2 Embankments with Geogrids and Cushion Layers

Figs. 2 and 3 show the geometrical scheme of the reinforced embankments. The only difference between the Types 1 and 2

embankments is the width of the cushioning layer. The cushioning layer is made of geocells filled with crushed stones of 5-13 mm in diameter. The geocells are of the TW-150M type, in which the height, width and length are 150 mm, 2650 mm and 800 mm, respectively, and are made of high density polyethylene (HDPE).

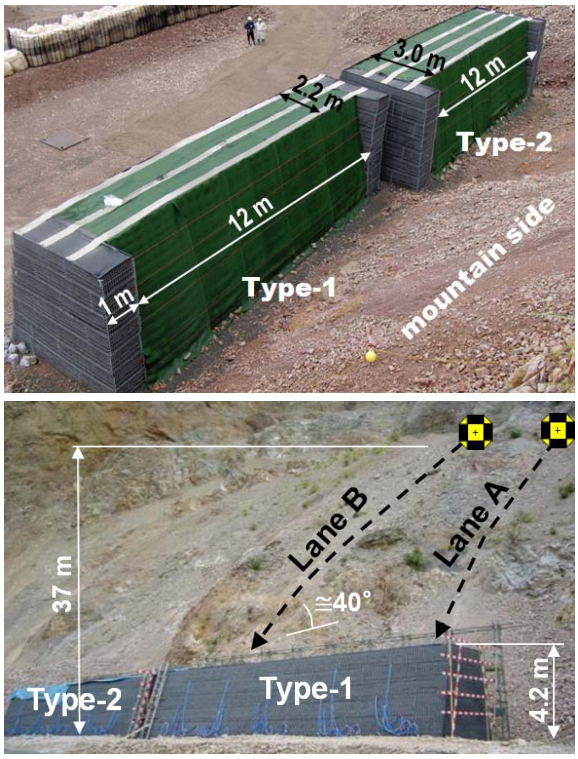

Fig. 2 Features of embankments and rock-slope lanes

Table 1 Physical properties of geogrids

Geogrid type	Polymer	Open size of strands (mm)	Tensile strength (kN/m)	Creep strength (kN/m)
RSGB*	HDPE	166 x 22	36.0	21.6
TX**	PP***	46.2	10.0	3.0

*unidirectivity, **quasi-isotropy, ***polypropylene

Table 2 Geotechnical properties of soil

Natural dry density γ_{dn}	15.4 kN/m^3
Natural water content w_n	13.7 %
Maximum dry density γ_{dmax}	16.6 kN/m^3
Optimum water content w_{opt}	17.8 %
Friction angle ϕ'_{cu}	25.1 degrees
Cohesion C'_{cu}	0 Pa
Classification: GFS	Gravel (62.4 %), Sand (21.1 %), Silt and clay (16.5 %)

Fig. 4 shows two kinds of geogrids, RSGB and TX, which are used in alternate layers of the embankment as shown in Fig. 3. Both kinds of geogrid act to reinforce embankments in the impact direction. Owing to its quasi-isotropy, the TX geogrid is expected to disperse the impact in the lateral direction of the wall embankment. Table 1 shows the physical properties of these geogrids. In order to close the embankment and to link the geogrid to itself, 6 mm and 8 mm diameter wire meshes are used for Type 1 and 2 embankments, respectively (see Fig. 5).

Table 2 shows the geotechnical properties of the soil used for the construction of the embankments.

2.3 RC Block and System of Measuring Instruments

Fig. 6 shows 5.2, 10.1, and 17.1 ton RC blocks covered with steel plates 6 mm thick. The shape of the blocks is based on the definition in ETAG-027 [3]. Two pieces are assembled into an RC block using six tendons.

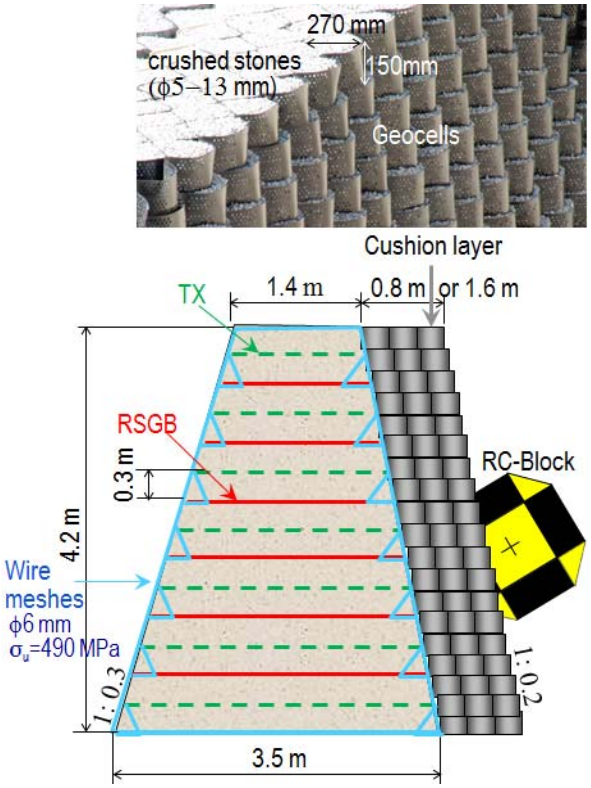

Fig. 3 Geometric scheme of embankment & cushion layer

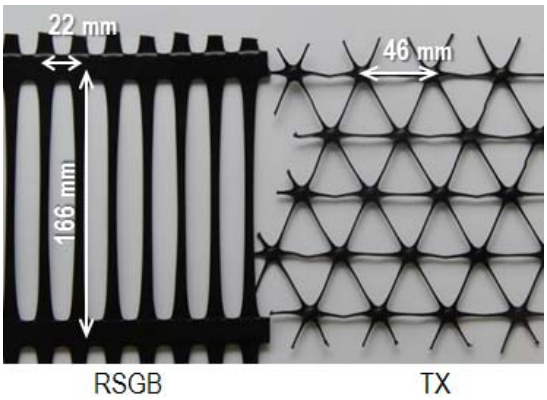

Fig. 4 Two kinds of geogrids, RSGB and TX

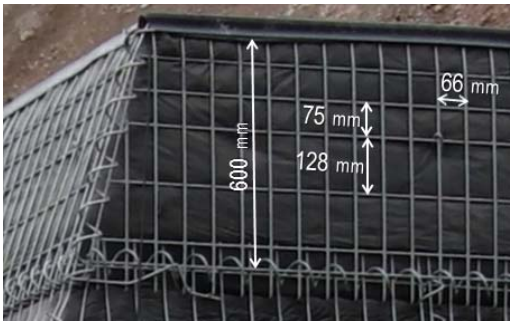

Fig. 5 Wire meshes

A triaxial accelerometer was set on the center of each RC block in order to measure the impact force of the block during a collision with the embankment. In case of the block rolling down the slope, no measurement cable, however, was available; therefore, an amplifier-recorder device and cushions were also put in the space provided inside each RC block, as shown in Fig. 7, and then the space lid was shut. The similar device consisting of six accelerometers and a computer control unit was integrated in an artificial boulder for use in rockfall protection experiments [8].

The motion of each RC block was recorded by high-speed cameras operating at 300 fps, and the acceleration of each RC-block was measured by the triaxial accelerometer device at 2000 Hz. The strains of geogrids were also measured for comparison with analytical solutions to be executed in future. These measuring instruments for acceleration and motion of the block rolling down were synchronized by a trigger signal through transceivers. It is the first time that this synchronized system has been introduced to a slope-rockfall experiment. The deformations of the embankment and the penetration were measured after impact.

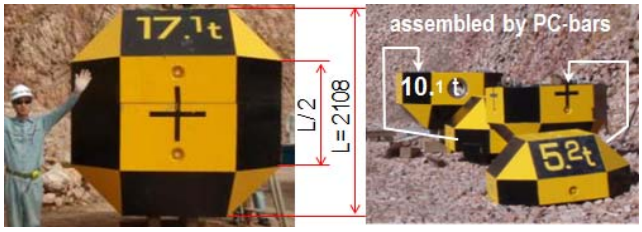

Fig. 6 RC-blocks of 17.1 ton, 10.1 ton and 5.2 ton

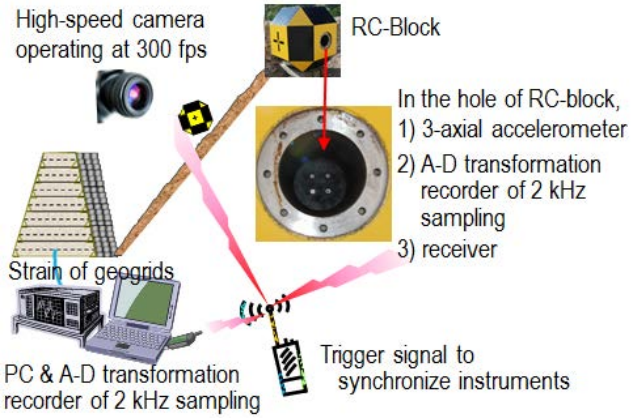

Fig. 7 System for synchronizing measuring instruments

3 TESTS PROCEDURES AND RESULTS

3.1 Test Conditions

Eight tests were conducted using two embankments. The test variables are shown in Table 3; *(a) CushionWidth, (b) Slope Lane, (c) Block Mass*, and *(d) Block Size*. The slope lanes of A and B are related to the embankment Types 1 and 2, respectively. The cushioning layers of Types 1 and 2 have been removed before test Nos. 4 and 8, respectively.

Table 3 Test conditions and results

Test No.	1.	2.	3.	4.	5.	6.	7.	8.
(a) Cushion Width (m)	0.8	0.8	0.8	---	1.6	1.6	1.6	---
(b) Slope Lane	A	A	A	A	B	B	B	B
(c) Block Mass M (ton)	5.2	10.1	17.1	10.1	17.1	17.1	17.1	17.1
(d) Block Size L (m)	1.41	1.77	2.11	1.77	2.11	2.11	2.11	2.11
(e) Contact Height H (m)	0.70	1.51	2.55	2.31	2.55	2.65	2.85	2.15
(f) Translation Velocity v_t (m/s)	16.4	14.5	14.4	15.7	13.9	14.0	11.1	16.3
(g) Angular Velocity v_r (rad/s)	11.8	10.7	7.1	12.1	9.3	10.1	10.5	9.7
(h) Translation Energy E_v (kJ)	697	1060	1763	1243	1655	1673	1053	2270
(i) Rotation Energy E_r (kJ)	89	221	274	284	401	477	514	439
(j) Impact Energy E (MJ)	0.79	1.28	2.04	1.53	2.06	2.15	1.57	2.71
(k) Max. Impact Force F_m (MN)	2.24	3.40	5.46	3.55	5.18	5.37	3.69	5.27
(l) Max. Protrusion Height δ_p (mm)	33	88	239	266	100	133	91	441
(m) Max. Depth of Crater δ_c (mm)	824	1127	1727	1565	760	1800	1444	1900

Fig. 8 RC-block trajectory by highspeed images of test No. 7

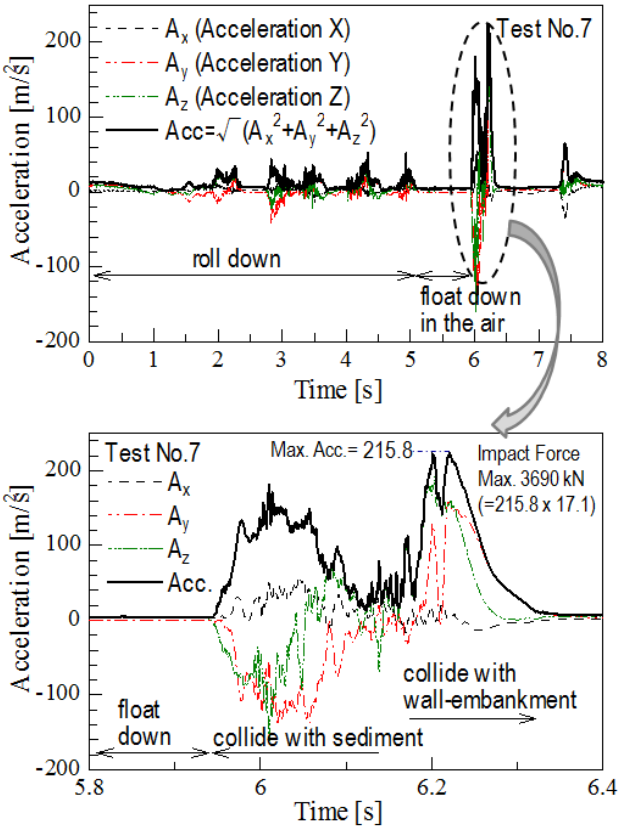

Fig. 9 Example of acceleration of RC block

3.2 Test Results

The test results for the parameters *(e)* through *(m)* are also presented in Table 3.

(e) Contact Height is the height of the penetration center of an RC block from the base of an embankment, measured after the impact.

(f) Translation Velocity and *(g) Angular Velocity* are estimated using high-speed images taken just before the impact of an RC block on an embankment. Fig. 8 shows the trajectory of an RC block and a composite image in which numerical values indicate the time in seconds and express the rotational direction of an RC block. It is possible for the rolling momentum of an RC block to carry it toward the top of an embankment after the initial collision. It might be dangerous for us to ignore the rolling motion of a rockfall in order to design an embankment. This boulder's rolling motion has been left out of the past experiments on not only rockfall protection embankments but also rockfall protection fences.

(j) Impact Energy is the sum of *(h) Translation Energy* and *(i) Rotation Energy*, which are calculated from *(f) Translation Velocity*, *(g) Rotation Velocity* and the mass and moment of inertia of the RC block. *(k) Maximum Impact Force* is calculated by multiplying the block's mass by its maximum root-mean-square acceleration. Fig. 9 shows an example of accelerations measured by a triaxial accelerometer and their root-mean-square. The contact time of an RC block with an embankment can be estimated from the high-speed camera's frame number at which the RC-block is observed coming into collision with the embankment, because the measuring instruments have been synchronized.

(l) Maximum Protrusion Height was measured horizontally on the downstream face of an embankment.

(m) Maximum Depth of a Crater was measured horizontally on the upstream face of an embankment.

Table 4 Observations & repairs after each test

No.	*the i-th* impact on specimen by a block	Observations & Repairs on C) Cushioning layer E) Embankment
1.	*1st* on Type-1 *M*=5.2 ton	C) was partially damaged, and repairs were made to carry out No. 2. E) was not damaged, and repairs were not needed.
2.	*2nd* on Type-1 *M*=10.1 ton	C) was damaged, and repairs were made to carry out No. 3. E) suffered slight protrusion on downstream face, and repairs were made.
3.	*3rd* on Type-1 *M*=17.1 ton	C) was damaged, and was removed to carry out No. 4. E) suffered wider and higher protrusion on downstream face. Wire-meshes were partially broken. Repairs were made to carry out No. 4.
4.	*4th* on Type-1R* *M*=10.1 ton	E) suffered wider and higher protrusion on downstream face. Wire-meshes were broken at many parts
5.	*1st* on Type-2 *M*=17.1 ton	C) was damaged, and repairs were made to carry out No. 6. E) suffered slight protrusion on downstream face, and repairs were made.
6	*2nd* on Type-2 *M*=17.1 ton	E) suffered progress of protrusion on downstream face, but repairs were not made.
7	*3rd* on Type-2 *M*=17.1 ton	C) was damaged, and was removed to carry out No. 8. E) suffered wider progress of protrusion on downstream face, but no repair was made.
8	*4th* on Type-2R* *M*=17.1 ton	E) suffered wider and higher protrusion on downstream face. Wire-meshes were broken at many parts, especially welded points.

R*: embankment without cushion layers.

3.3 Discussion on Test Results

As a supplement to Table 3, Table 4 shows observations of cushions and embankments after each test. It also indicates whether they were repaired or not. Although there is a large difference in the damage suffered by the embankments among the tests, even a huge RC block weighing 17.1 tons and carrying 2.71 MJ of energy was stopped. Moreover, no embankment collapse occurred under the impact of RC blocks rolling down an actual slope.

It is difficult in practice to control the trajectory of the blocks' direct impact on the embankment because of blocks'

geometry, variations in the slope and difficulty in controlling the exact starting conditions. In many tests, RC blocks with higher kinetic energies collided with sediment between the embankment and the edge of the slope first. Then, after they had already dissipated a part of their kinetic energy, they collided with the embankment.

Consequently, the translation velocities shown in Table 3 vary from 11.1 to 16.3 m/s, and are different from each other even in test Nos. 5, 6, 7 and 8, which use identical blocks rolling down on the same slope. Similarly, the angular velocities vary from 7.1 to 12.1 radian/s. Therefore, the impact energies range from 1.57 to 2.71 MJ even in those tests with identical conditions.

Using high-speed images taken just before the impact of an RC block on the sediment, the kinetic energies in test Nos. 5, 6, 7 and 8 can be estimated at 5.72, 5.24, 3.25, and 4.61 MJ, respectively. Unfortunately, on average, more than 50% of the kinetic energy was lost, as compared with the impact energies in Table 3 due to the energy dissipation during block's collision with the sediment.

Figs. 10 and 11 show the deformation of embankments and cushion layers after test Nos. 7 and 8, respectively. The cushion layer is indeed damaged in exchange for playing the role of an absorber for the embankment but can be rebuilt easily. On the contrary it is not so easy to repair the embankment damaged by the direct impact of a boulder. Therefore a cushion layer is effective in not only protecting embankments but also reducing life cycle costs.

Due to a vertical rockfall onto a sand cushion the maximum impact force, F_{max}, can be predicted by (1) that is shown in the rockfall mitigation handbook [1].

$$F_{\max} = 2.108\left(M \cdot g\right)^{2/3} \cdot \lambda^{2/5} \cdot H^{3/5} \quad (1)$$

where F_{max} (kN) = maximum impact force originally based on Herz's theory; M (ton) = mass of a rockfall; g (m/s^2) = gravity; λ (kN/m^2) = Lame's constant of a sand cushion; H (m) = fall-height.

The corresponding height, H, can be evaluated by the equation, $H=E/(Mg)$, if the impact energy, E, and the mass, M, are given. In this case, *(h) Translation Energy*, E_v in Table 3, should be applied to (1), since the equation is based on translational impact motion. Therefore Fig. 12 shows the relationship between the translation energy and the maximum impact forces which were measured in the experiments and/or predicted by (1) depending on Lame's constants of 1000, 1500 and 2000 kN/m^2. The prediction by (1) might be useful if it is important to predict the maximum impact force in designing structures. Under a huge rockfall being less probable to occur, the reasonable design for the rockfall protection structure should, however, be based on the allowable impact energy with avoiding the fatal damage.

Fig. 13 shows the relationship between *(j) Total-Impact-Energy* and *(k) Maximum-Impact-Force*. The value in parentheses in the figure indicates *(l) Maximum-Protrusion-Height* measured horizontally on the downstream face of embankments. There is a linear relationship between them, except in test No. 4 and, especially, in test No. 8. It seems that the impact force for embankment Type-1, with the single cushioning layer, tends to be slightly larger than that for embankment Type 2 with the double layer. Therefore, the cushioning layer does indeed play the role of a shock absorber. The impact force of the embankment without a cushion corresponding with test Nos. 4 and 8 seems very small, though the protrusion is very large. In this case, the impact energy is too high for an embankment to keep a steady state.

Fig. 10 After the impact of test No. 7

Fig. 11 After the impact of test No. 8

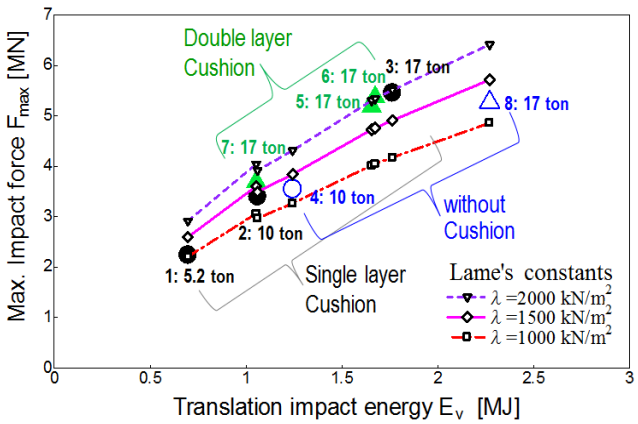

Fig. 12 Impact forces by prediction and measurement

Fig. 14 shows the relationship between *(j) Impact Energy* and *(l) Maximum Protrusion Height* on the downstream face of embankments. The amount of protrusion can be an index for the allowable impact energy not to bring the fatal damage for an embankment, though the relationship between protrusion and impact energy depends on structural components, i.e., with or without cushioning layers. However, unfortunately it

has not been decided how amount of protrusion is related to the fatal damage of an embankment.

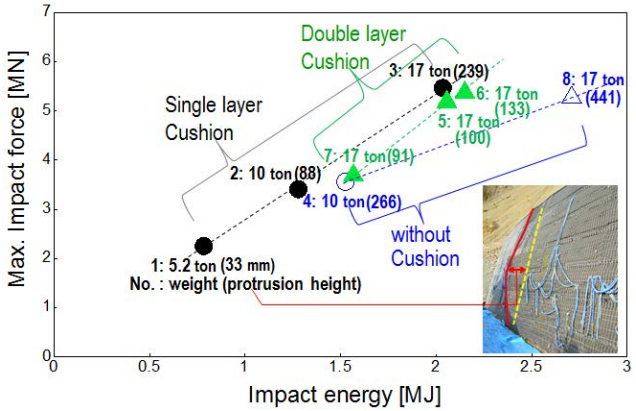

Fig. 13 Relationship between impact energy and force

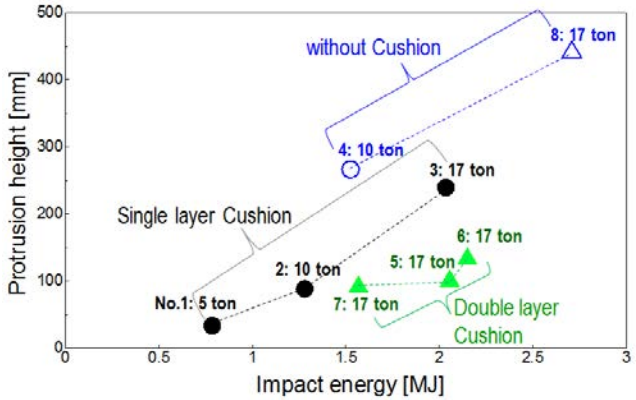

Fig. 14 Protrusion height of embankments

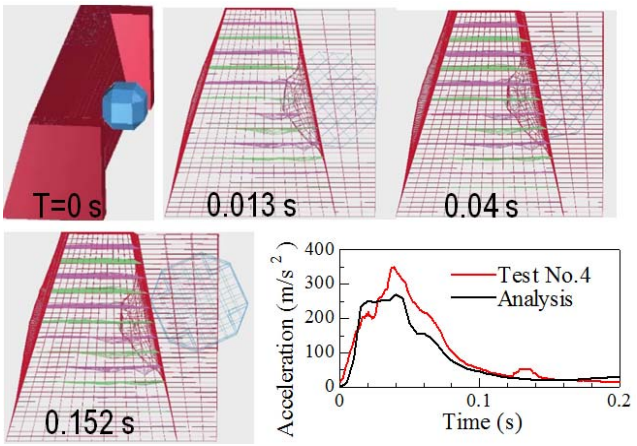

Fig. 15 Example of simulation analysis in progress

The measured data such as the impact force, the strain of geogrids and residual deformation will contribute to the calibration for the simulation analysis on tested embankments. The analytical approach is in progress using LS-DYNA which is a transient and dynamic finite element program. Fig. 15 shows an example of simulation analysis of test No. 4. The analytical acceleration of an RC block is in good agreement with the experimental result.

4 CONCLUSION

Slope-rockfall tests were carried out on rockfall protection embankments reinforced with geogrids and cushioning layers. The impact energies in the tests were estimated at 0.79 to 2.71 MJ just before rolling RC blocks collided against embankments. Furthermore the synchronized measuring instruments were introduced in order to measure the impact force and motion of the RC block rolling down a slope.

Even embankment without a cushioning layer has stopped the huge RC block weighing 17.1 tons and carrying 2.71 MJ of energy. The cushioning layer set on the upstream side of an embankment is, however, effective in reducing the deformation of embankments. Consequently it will be possible to repair an embankment at low cost.

5 ACKNOWLEDGMENT

The authors wish to thank the Association of Rock Geo-Bank for the financial support to the experiments. Further thanks go to Tajima T., Shimada M., Murata Y., Akinaga T., Watanabe S., Namba M. and Tohda M. who have cooperated with authors to carry out the experiments.

6 REFERENCES

[1] JRA (Japan Road Association), “Rockfall Mitigation Handbook (in Japanese),” Maruzen, 2000.

[2] GERBER W., “Guideline for the approval of rockfall protection kits,” Swiss Agency for the Environment, Forests and Landscape (SAEFL), 2001.

[3] ETAG-027, “Guideline for European Technical Approval of Falling Rock Protection Kits,” European Organization for Technical Approvals (EOTA), 2008.

[4] Peila D., Oggeri C., and Castiglia C., “Ground reinforced embankments for rockfall protection: design and evaluation of full scale tests,” Landslides, Vol.4(3), Springer-Verlag, Sep. 2007, pp.255-265.

[5] Burroughs K., Henson H. and Jiang S., “Full scale geotextile rock barrier wall testing, analysis and prediction,” in Proc. Geosynthetics'93, IGS, Vancouver, 1993, pp.959-970.

[6] Obata Y., Fuchigami M., Yokota Y., Nomura T. and Yoshida H., “Actual Rolling Rock Test of Rockfall Protection MSE-Wall,” J. of Geosynthetics (in Japanese), Vol.13, JCIGS, Dec. 1998, pp.60-68.

[7] Peila D., Castiglia C., Oggeri C., Guasti G., Recalcati P. and Sassudelli F., “Full scale tests on geogrid reinforced embankments for rock fall protection,” in Proc. Second European Geosynthetics Conference, Bologna, 2000, pp.15-18.

[8] Volkwein A, Fritschi B, Schaedler S, and Grassl H., “Posterior trajectory analysis of an artificial instrumented boulder,” Geophysical Research Abstracts, Vol.8, EGU06-A-03856, 2006, Poster.

International Journal of GEOMATE , Oct. 2011, Vol. 1, No.1 (Sl. No. 1)
MS No. 1e received September 1, 2011, and reviewed under GEOMATE publication policies.

Corresponding Author: Koji Maegawa